Lens-based Light Collector Design Characteristics

John McGill and Roy Schwitters

November, 1996

This note summaries results of our design studies[1, 2] of lens-based light collectors for the HERA-B RICH system. Two basic designs are considered:

X4: Light collected over a $36 \times 36\,\mathrm{mm}^2$ square field lens and transported to a $18 \times 18\,\mathrm{mm}^2$ photocathode surface.

X9: Light collected over a $54 \times 54\,\mathrm{mm}^2$ square field lens and transported to a $18 \times 18\,\mathrm{mm}^2$ photocathode surface.

A drawing of the X4 design with a representative cone of rays is shown in Figure 1. All lenses are assumed to be made from a UV-transmitting acrylic material, such as Acrylite, with an index of refraction, $n = 1.49$. The positions and focal lengths of the lenses used in each design are given in Table 1.

Rays were traced through all optical surfaces*, using standard Fresnel formulae, to determine reflection losses. Appropriate apertures were imposed to determine geometric losses. The total path-length in the lenses was computed to determine absorption losses. In all cases, photons were assumed to be distributed uniformly in position over the entrance face of the field lens. The directions of the incident photons were assumed to fall uniformly within a cone of polar angles, $78 \rightarrow 104\,\mathrm{mr}$ (twice the Čerenkov angle). The angle between the axis of this cone and the normal to the field lens is called the "tilt-angle"; it was varied in the studies to determine the effect on collection efficiency for particle tracks that do not project back to the center-of-curvature of the focusing mirrors—arising from low-momentum tracks and the vertical tilt of the spherical mirrors. For reference, the tilt used in the present study was taken to be *around* the x-axis†.

The accumulation of losses due to apertures, reflections, and absorption through the light collector systems is tabulated in Table 2. The reflections differ slightly from the "canonical" 3.8% loss per interface because of the curved surfaces of the lenses and the particular distribution of angles of the rays as they strike the lens faces. The reflection losses are actually slightly reduced in our case because many of the rays cross the curved condenser-lens surfaces at angles near the Brewster angle.

*Typically, 10,000 rays were generated in each separate calculation.

†x,y form an orthogonal coordinate system in the plane of the field lens, with axes parallel to the square sides of this lens.

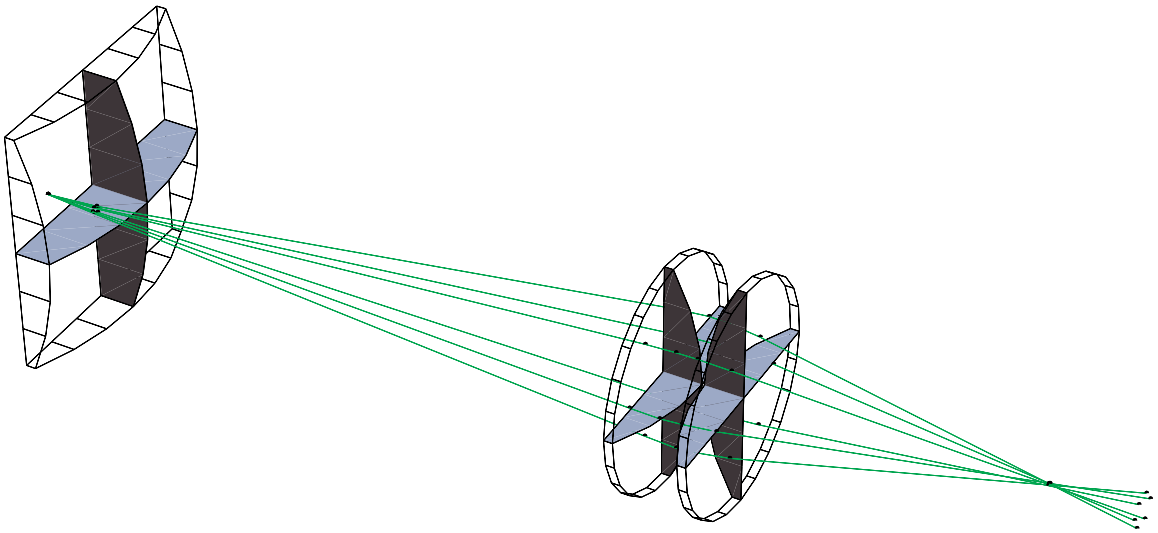

Figure 1: Perspective drawing of the X4 light collector design with a typical cone of rays (half-angle of cone = 2×Čerenkov angle; tilt-angle = 0).

Design	**Object**	**Position** (mm)	**Thickness** (mm)	**Focal length** (mm)
X4	field lens	0	8.9	91.6
	1st condenser	89.7	5.6	61.1
	2nd condenser	95.4	5.6	61.1
	cathode screen	140.3		
X9	field lens	0	12.9	137.5
	1st condenser	134.8	10.1	68.7
	2nd condenser	144.9	10.1	68.7
	cathode screen	189.9		

Table 1: Positions and focal lengths of lenses used for light collectors.

Design	**Depth** (behind element)	**Survival Fraction**		**Path-length** (mm)
		Geometric	**Reflections**	
X4	field lens	.992	.922	6.4
	1st condenser	.978	.857	10.9
	2nd condenser	.972	.796	15.3
	cathode screen	.954	.796	15.4
X9	field lens	.990	.922	9.1
	1st condenser	.973	.863	16.8
	2nd condenser	.975	.805	24.6
	cathode screen	.975	.805	24.6

Table 2: Accumulated efficiency factors at various depths along the collector for zero tilt angle.

Design	**Tilt** (mr)	**Survival Fraction**		**Path-length** (mm)	**Collection Efficiency**	**Photon Yield**
		Geom.	**Refl.**			
X4	0	.954	.796	15.4	.605	35.8
	50	.901	.797	15.1	.574	34.0
	100	.696	.800	14.7	.447	26.4
X9	0	.975	.805	24.6	.581	34.4
	50	.949	.809	23.7	.573	33.9
	100	.663	.809	23.7	.400	23.7

Table 3: Summary of light collection efficiency calculations for various values of tilt-angle. The photon yield is the average number of detected photo-electrons for $\beta = 1$ tracks.

Absorption losses were computed by convoluting the wavelength-dependent transmissivity (computed from the average path-length) of the lens material with the incident spectrum and the quantum efficiency expected for the Hamamatsu phototubes. In our model, a *perfect* light collector would yield 59.2 photo-electrons per $\beta = 1$ track[‡].

A summary of results on collection efficiency is given in Table 3. For moderate tilt-angles, the geometric efficiency is greater than 90% in both designs. The reflections are close to what one would expect from the six optical interfaces in this design, reduced slightly as described above. At larger tilt angles, the survival fractions due to reflections and absorption actually increase, partially compensating for the reduced geometric efficiency.

We conclude from this table that, for tilt-angles below about 50 mr, the average col-

[‡]The model for photon yields uses conservative estimates for the losses due to gaps between active elements of the RICH system and other factors, not directly related to light collection. The equivalent number of photo-electrons for perfect detectors with no gaps would be 70.

Design	Tilt	Magnification		Optical Error	
	(mr)	$x_{cathode}/x_{in}$	$y_{cathode}/y_{in}$	σ_x (mm)	σ_y (mm)
X4	0	-0.497	-0.496	0.3	0.3
	50	-0.501	-0.506	0.4	0.7
	100	-0.515	-0.537	0.8	1.6
X9	0	-0.328	-0.328	0.6	0.6
	50	-0.334	-0.348	1.1	2.2
	100	-0.364	-0.407	2.9	6.1

Table 4: Optical performance characteristics for various values of tilt-angle.

lection efficiency will be uniform at the level of a few %. Under conservative estimates, both the X4 and X9 designs will yield more than 30 *detected* photo-electrons for $\beta = 1$ tracks. It is important to note that a 50 mr tilt corresponds to incidence angles up to 150 mr, because the efficiencies quoted here are averaged over the Čerenkov cone. At larger tilt-angles, however, rays will begin to miss the condenser doublet, incurring significantly larger geometric losses.

The optical performance of these collectors is summarized in Table 4. Magnification is taken from the average slope in the correlation between input locations of the ray and the final position on the cathode screen. The optical error is defined as the RMS difference between the position on the field lens for the ray and that projected, assuming linear optics with the average magnification for the particular design and cathode pad region. These optical errors are to be compared with the RMS cell size, $c/\sqrt{12}$, assumed for a particular arrangement of phototube and optical magnification. For M16 tubes with X4 optics, the corresponding RMS cell size is 2.6 mm; that for M4 tubes with X9 optics is 7.8 mm.

The average magnifications and optical errors are seen to grow with increasing tilt-angle. The asymmetry in the tables arises because the tilt is about the x-axis.

The Hamamatsu M16 phototubes have three classes of cathode pads, depending on their relative position within the tube. We identify these as *center*, *edge*, and *corner* cells. Figure 2 shows the layout of the M16 photo-cathode, with the types of pads indicated. There are four center cells, eight edge cells, and four corner cells.

The performance characteristics of the different types of cells is given in Table 5. For this study, the edge cell chosen was on a side of the array that is parallel to the y-axis, accounting for the small x-y asymmetry in optical error indicated in the table. As noted previously, the loss in geometric efficiency in moving from center cells to edge and corner cells is partially compensated by reduced absorption, leading to cell-to-cell variations in average collection efficiency at the 5% level or less.

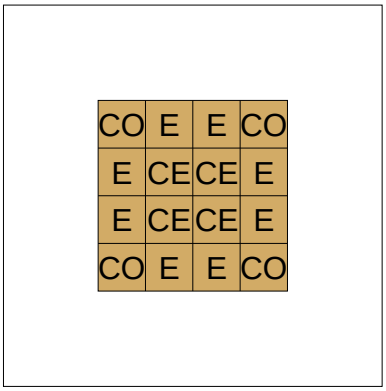

Figure 2: Layout of the Hamamatsu M16 photomultiplier, indicating the different types of cathode pads considered in the performance studies. The three distinct types of cathode pads are called, center (CE), edge (E), and corner (CO).

Design	**Cathode Pad**	**Geometric Efficiency**	**Path-length** (mm)	**Collection Efficiency**	**Optical Error**	
					σ_x (mm)	σ_y (mm)
X4	corner	.896	13.0	.577	0.5	0.5
	edge	.960	15.4	.609	0.4	0.2
	center	1.000	17.6	.622	0.1	0.1
X9	corner	.913	20.7	.557	0.8	0.8
	edge	.991	24.6	.591	0.6	0.4
	center	1.000	28.1	.582	0.2	0.2

Table 5: Light collector performance for the different types of cathode pads. Results shown for zero tilt angle.

References

[1] J. McGill and R. F. Schwitters, *Design Study for M16 Light Collectors*, HERA-B Note 96-263, September, 1996.

[2] J. McGill and R. F. Schwitters, *Further Report on Telescope Design for RICH Light Collection*, HERA-B Note 96-264, October, 1996.